

Identification and functional characterization of the human *ether-a-go-go*-related gene Q738X mutant associated with hereditary long QT syndrome type 2

SHENG-NA HAN^{1*}, SONG-HUA YANG^{2*}, YU ZHANG³, XIAO-YAN SUN¹, YAN-YAN DUAN¹, XIANG-JIE HU¹, TIAN-LI FAN¹, CHEN-ZHENG HUANG¹, GE YANG², ZHAO ZHANG⁴ and LIRONG ZHANG¹

¹Department of Pharmacology, School of Medicine, ²The First Affiliated Hospital, Zhengzhou University;

³Pharmacy College of Zhengzhou Railway Vocational and Technical College, Zhengzhou, Henan;

⁴Jiangsu Province Key Laboratory for Molecular Medical Biotechnology, College of Life Science, Nanjing Normal University, Nanjing, Jiangsu, P.R. China

Received March 7, 2014; Accepted June 23, 2014

DOI: 10.3892/ijmm.2014.1827

Abstract. QT interval prolongation, a risk factor for arrhythmias, may be associated with genetic variants in genes governing cardiac repolarization. Long QT syndrome type 2 (LQT2) is caused by mutations in the human *ether-a-go-go*-related gene (hERG). This gene encodes a voltage-gated potassium channel comprised of 4 subunits, and the formation of functional channels requires the proper assembly of these 4 subunits. In the present study, we investigated the role of the LQT2 mutation, Q738X, which causes truncation of the C-terminus of hERG channels, in the assembly and function of hERG channels. When expressed in HEK293 cells, Q738X did not generate an hERG current. The co-expression of Q738X with wild-type (WT)-hERG did not cause the dominant-negative suppression of the WT-hERG current. Western blot analysis and confocal microscopy revealed that the Q738X mutation caused defective trafficking of hERG channel proteins. Co-immunoprecipitation demonstrated that Q738X did not exhibit dominant-negative effects due to the failure of the mutant and WT subunits to co-assemble. In conclusion, the functional loss caused by the Q738X mutation in hERG K⁺ channels may be attributed to the disruption of tetrameric assembly.

Introduction

Hereditary long QT syndrome (LQTS) is a genetic disorder caused by mutations in one or more of a number of ion channel

subunits expressed in the heart, which can lead to ventricular arrhythmias, syncope and sudden death (1). The human *ether-a-go-go*-related gene (hERG) encodes the α -subunit of the rapidly activating delayed rectifier K⁺ channel (I_{Kr}). In the mammalian heart, this channel is critical to cardiac action potential and repolarization (2). Mutations in the hERG gene are one of the principal causes of congenital LQTS (3). Over 300 hERG mutations have been identified to date (<http://www.fsm.it/cardmoc/>). A variety of mechanisms have been suggested to underlie the dysfunction of the hERG channel in these mutants, including the failure of the mutant channels to reach the cell surface due to problems with trafficking, defective gating or permeation, the formation of dysfunctional channels and dominant-negative suppression of the function of wild-type channels (4). In addition, truncated nonsense LQT2 mutants residing at the C-terminus have been shown to arise from insertion or deletion mutations producing premature stop codons; however, the mechanisms underlying hERG channel dysfunction in association with C-terminal mutations have not yet been fully characterized (5). In order to gain a better understanding of the function of hERG channels, it is important to first understand the mechanisms through which each of these mutations cause hERG channel dysfunctions; this will also allow us to develop more effective therapies for disorders involving hERG channel dysfunctions (6). A previous study (7) identified Q738X, a nonsense mutation (c.C2212T and p.Q738X) in the C-terminus of the hERG protein in a Japanese LQT2 patient. However, the mechanisms through which the Q738X mutation affects hERG channel dysfunction have not been elucidated.

In the present study, we sought to characterize the functional consequences of the Q738X mutation. Our results suggest that the functional loss caused by the Q738X mutation in hERG K⁺ channels is attributable to the disruption of tetrameric assembly.

Materials and methods

Site-directed mutagenesis. The wild-type (WT)-hERG cDNA subcloned into a pCGI-EGFP vector was kindly provided by

Correspondence to: Professor Lirong Zhang, Department of Pharmacology, School of Medicine, Zhengzhou University, 100 Science Road, Zhengzhou, Henan 450001, P.R. China
E-mail: zhanglirongzzu@126.com

*Contributed equally

Key words: human *ether-a-go-go*-related gene, long QT syndrome, QT interval, mutation, trafficking protein, tetramer assembly

Dr Zhao Zhang (College of Life Science, Nanjing Normal University, Nanjing, China). Mutant pCGI-EGFP-Q738X was constructed by overlap extension PCR with mutagenesis oligonucleotide primers and verified by DNA sequencing. The primer sequences were as follows: outer primers, 5'-GCG CCT CGA GGA GTA CTT C-3' (5'-end) and 5'-GAG GGA GCT CCT GGT ACT GG-3' (3'-end); and internal primers, 5'-TGG CCC CTC GGA AGG GTT TGC AGT GCT ACA GCA GTG AGC GG TTC-3' (5'-end) and 5'-GCC TGC ACC TGA ACC GCT CAC TGC TGT AGCACT GCA AAC CCT TC-3' (3'-end) (the underlined letters indicate the site of mutation). pCGI-WT-hERG and pCGI-Q738X-hERG were verified by direct sequencing. The plasmid DNA for mammalian expression was amplified in *Escherichia coli* DH5 α competent cells and was isolated from the bacterial cells using the EndoFree Plasmid Maxi kit (KeyGen Biotech Co., Ltd., Nanjing, China). The cDNA concentration was quantified by UV absorption.

Cell culture and transfection. HEK293 cells (obtained from the Institute of Biochemistry and Cell Biology, Shanghai, China) were cultured in Dulbecco's modified Eagle's medium (DMEM) supplemented with 10% fetal bovine serum (FBS) and 1% penicillin-streptomycin in a humidified 5% CO₂ incubator at 37°C. Transient transfections were performed using Lipofectamine 2000 according to the manufacturer's instructions (Invitrogen, Carlsbad, CA, USA).

Electrophysiological recordings. hERG currents were recorded by the whole-cell patch clamp technique at room temperature (18–23°C) as previously described (8). GFP-positive cells were visually selected using an epifluorescence system (Olympus, Tokyo, Japan). Recordings were obtained using a HEKA EPC-10 amplifier with Pulse 8.67 software (HEKA Elektronik Inc., Mahone Bay, NS, Canada). Pipettes were pulled from 1.5-mm borosilicate glass capillary tubes using a micropipette puller (P-87; Sutter Instrument, Novato, CA, USA). The cells were superfused with bath solution containing 140 mM NaCl, 5.4 mM KCl, 1.8 mM CaCl₂, 1 mM MgCl₂, 10 mM glucose and 10 mM HEPES (pH 7.4, adjusted with NaOH). Pipettes with tip resistances of 2–5 M Ω were filled with an internal solution containing 130 mM KCl, 1 mM MgCl₂, 5 mM EGTA, 5 mM Na₂ATP and 10 mM HEPES (pH 7.2, adjusted with KOH). Cell capacitance and series resistance were routinely compensated to reduce the voltage error (limited to 5 mV in an experiment). A giga-ohm (G Ω) seal resistance was achieved in all experiments. The kinetic characteristics of the hERG channel were recorded as previously described (8,9).

Western blot analysis. The antibodies used in the present study have been previously described (10). Briefly, the cells were solubilized in ice-cold RIPA lysis buffer [50 mM Tris-HCl (pH 7.5), 150 mM NaCl, 1% deoxycholate, 1% Triton X-100, 2 mM EDTA, 0.1% SDS and 50 mM NaF]. Proteins were subjected to SDS-PAGE and then electrophoretically transferred onto PVDF membranes. After blocking, the membranes were incubated with rabbit anti-hERG antibodies (1:200; Alomone, Jerusalem, Israel) in 5% non-fat dry milk/TBST overnight. The membranes were then incubated with goat anti-rabbit horseradish peroxidase-conjugated secondary anti-

bodies (1:10,000; Santa Cruz Biotechnology, Santa Cruz, CA, USA) in TBST for 1 h. Signals were detected using an ECL detection kit.

Confocal microscopy. The HEK293 cells were transiently transfected with the different plasmids (WT, Q738X or WT/Q738X). After 36–48 h, the transfected cells were fixed in 4% paraformaldehyde, made permeable with 0.1% Triton X-100, and were pre-blocked with 2% bovine serum albumin at room temperature. The cells were subsequently incubated with rabbit polyclonal anti-hERG antibodies (1:50; Alomone) or chicken polyclonal anti-calreticulin antibodies (1:50; Abcam, Cambridge, MA, USA) overnight at 4°C, followed by incubation with FITC-conjugated goat anti-rabbit IgG secondary antibodies (1:100; Bioss Biotech Co., Ltd., Beijing, China) and Alexa Fluor-conjugated goat anti-chicken IgG secondary antibodies (1:100; Invitrogen) at 37°C for 2 h. Stained cells were viewed using a confocal laser scanning microscope (Olympus).

Co-immunoprecipitation. In order to quantify the WT/Q738X interactions, the Flag epitope (DYKDDDDK) and the Myc epitope (EQKLISEEDL) were introduced at the N-terminus of pCGI-hERG-WT and pCGI-hERG-Q738X, using PCR-based mutagenesis. Co-transfected cells (Flag-tagged WT/Myc-tagged Q738X, Flag-tagged WT/WT, Myc-tagged Q738X/Q738X) were washed with ice-cold PBS and incubated in lysis buffer (0.5% Nonidet P-40, 75 mM NaCl, and 50 mM Tris, pH 8.0) plus a protease inhibitor mixture (Roche Applied Science, Indianapolis, IN, USA) for 15 min. Protein samples (5 μ g) were incubated overnight at 4°C with either mouse anti-Flag antibodies (1:100; Cell Signaling Technology, Danvers, MA, USA) or rabbit anti-Myc antibodies (1:250; Cell Signaling Technology). The antigen-antibody complexes were isolated with protein A-agarose beads (Roche Applied Science) and were washed with RIPA lysis buffer. The immunoprecipitated proteins were subjected to SDS-PAGE, transferred onto PVDF membranes, and detected by western blot analysis with corresponding antibodies.

Statistical analysis. Data are presented as the means \pm SEM. Data analysis and drawings were generated using SPSS version 11.0 software (SPSS Inc., Chicago, IL, USA) and Origin 6.0 software (MicroCal Inc., Northampton, MA, USA). Statistical differences were evaluated by unpaired or paired t-tests and were considered significant at $P < 0.05$.

Results

Electrophysiological characteristics of the Q738X channel. Fig. 1 shows hERG current traces from the HEK293 cells transfected with plasmids expressing WT (4 μ g), WT (2 μ g), Q738X (4 μ g) or WT/Q738X (2 μ g each) constructs. Time-dependent outward K⁺ currents were elicited by depolarizing steps between -50 and +60 mV with a 10-mV step increment from a holding potential of -80 mV, followed by repolarization to -40 mV to produce tail currents. Fig. 1A and B shows representative currents of the cells expressing WT-hERG (4 and 2 μ g, respectively). By contrast, the cells expressing the Q738X mutant alone did not produce any measurable currents (Fig. 1C).

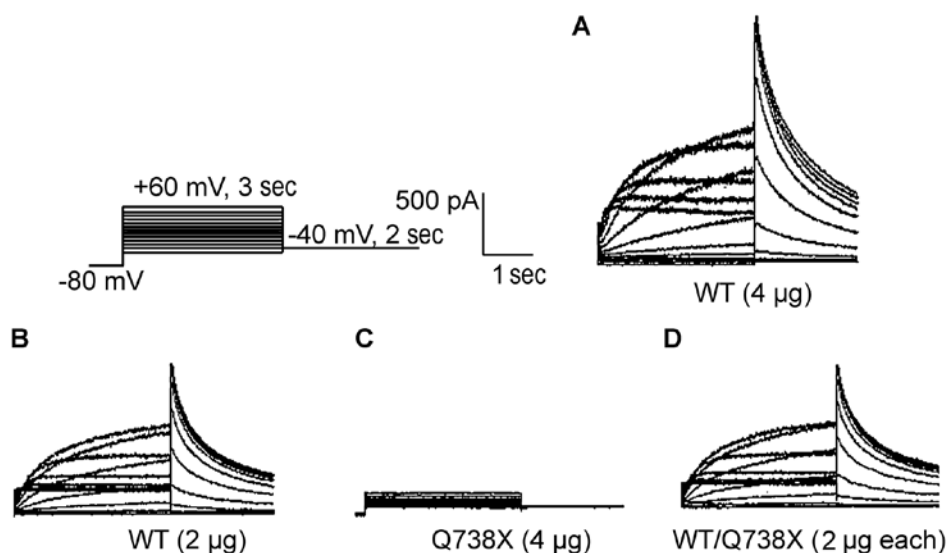


Figure 1. Representative current in HEK293 cells transfected with different human *ether-a-go-go-related gene* (hERG) plasmids. (A) Wild-type (WT) (4 μ g). (B) WT (2 μ g). (C) Q738X (4 μ g). (D) WT/Q738X (2 μ g each). Currents were elicited from a holding potential of -80 mV by depolarizing pulses from -50 to +60 mV with a 10-mV step increment and subsequent repolarization to -40 mV.

To mimic the heterozygous status that occurs in the patient and to assess the interaction between WT and mutant Q738X proteins, the HEK-293 cells were transiently co-transfected with WT and Q738X constructs at a 1:1 ratio (2 μ g each). These cells displayed significantly smaller outward currents compared with those transfected with 4 μ g WT hERG, but were similar to those transfected with 2 μ g WT hERG (Fig. 1D). These results demonstrated that the co-expression of WT and Q738X constructs reduced hERG current densities by approximately 50%.

Fig. 2A and B displays the current-voltage (I-V) relationships of the cells expressing WT (4 μ g) and WT/Q738X (2 μ g each) channels. The maximal current density was observed at 10 mV in the cells expressing the WT or WT/Q738X channels. The maximal current density was 18.5 \pm 1.1 pA/pF for WT/Q738X and 44.5 \pm 4.1 pA/pF for WT alone (P <0.05; Fig. 2A). The peak tail current density was 26.2 \pm 3.5 pA/pF for WT/Q738X and 59.9 \pm 3.2 pA/pF for WT alone (P <0.05; Fig. 2B). Furthermore, the current densities of the WT (2 μ g) or WT/Q738X (2 μ g each) channels did not differ significantly (P >0.05).

The normalized tail currents of the WT (4 μ g) and WT/Q738X (2 μ g each) channels were plotted as a function of the test potential and then fitted to a Boltzmann function. As shown in Fig. 2C, the voltage required for the WT channels to achieve half activation ($V_{1/2}$) was -5.4 \pm 0.1 mV, which did not differ from the corresponding value of -5.8 \pm 0.5 mV for WT/Q738X (P >0.05). The slope factors (k) were 9.8 \pm 0.1 and 10.8 \pm 0.4 mV (P >0.05), respectively. Thus, the voltage dependence of hERG channel activation was not affected by the Q738X mutation.

Steady-state inactivation was analyzed by application of test potentials between -130 and 20 mV in 10-mV increments for 20 msec after a depolarizing pulse to 20 mV for 4 sec, followed by application of a test pulse of 20 mV for 500 msec. The voltage was then returned to the -80-mV holding potential (Fig. 2D, inset). The inset shows representative current traces recorded from the HEK293 cells transfected with WT/Q738X (2 μ g each). Cells expressing the WT or WT/Q738X channels

did not differ in voltage to achieve $V_{1/2}$ (-45.0 \pm 1.0 vs. -46.1 \pm 1.0 mV; P >0.05) or slope factor k (24.5 \pm 0.9 vs. 24.8 \pm 0.9 mV; Fig. 2D). Therefore, the Q738X mutation did not alter the steady-state inactivation of the hERG channel.

Analysis of the deactivation time course was conducted by application of long hyperpolarizing test pulses following a depolarizing conditioning pulse. Subsequently, deactivating currents during test pulses were fitted to a double exponential function. The fast and slow time constants for Q738X/WT did not differ from those of the WT at all test potentials (data not shown).

To further examine the effects of Q738X on WT, we transiently transfected the cells with WT and Q738X cDNA at different ratios, including 4:0, 3:1, 1:3 and 0:4 (the total quantity of WT and Q738X cDNA was held constant). The currents from the cells co-expressing WT/Q738X decreased gradually with increasing amounts of Q738X cDNA (data not shown). These results indicated that the Q738X mutation did not result in the dominant-negative suppression of WT channels.

Q738X is a trafficking-deficient mutation. Western blot analysis was used to investigate the mechanisms involved in the dysfunction of mutant hERG channels. As shown in Fig. 3A, the expression of the WT protein yielded 2 protein bands: a 135-kDa lower band representing the endoplasmic reticulum (ER)-localized core-glycosylated immature form of the channel protein and a 155-kDa upper band, representing the plasma membrane-localized complex-glycosylated mature form of the channel protein. A truncated hERG protein of approximately 80 kDa was expressed in the cells having the Q738X mutation.

To further investigate the subcellular localization of WT, Q738X and WT/Q738X proteins, double immunofluorescence staining of hERG channels and the ER marker protein, calreticulin, was used (Fig. 3B). The transfected HEK293 cells were co-stained with antibodies targeting hERG (anti-hERG; left column) and calreticulin (anti-calreticulin; middle column). No hERG staining was observed in the non-transfected HEK-293

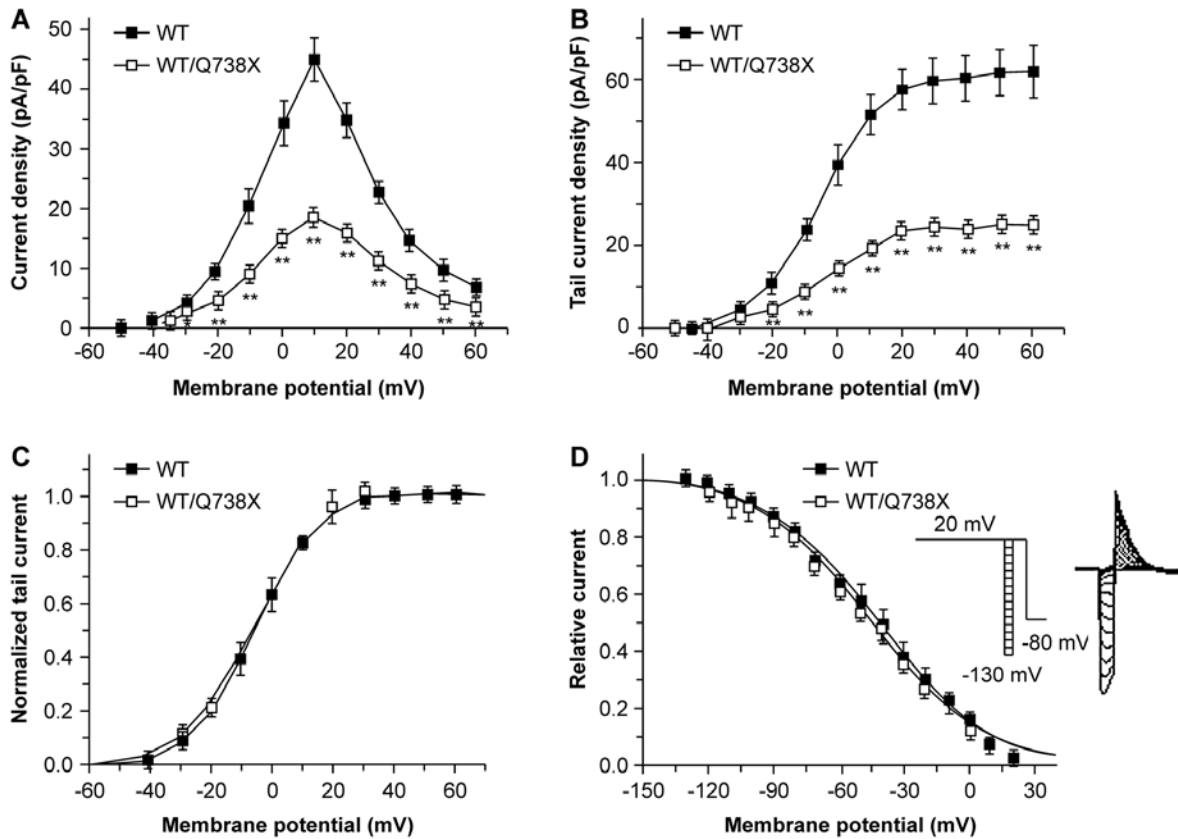


Figure 2. Voltage dependence of human *ether-a-go-go*-related gene (hERG) channel activation for wild-type (WT)-hERG and WT/Q738X-hERG. (A) Current-voltage (I-V) relationships for peak currents during test pulses. (B) I-V relationships for amplitudes of tail currents recorded during test pulses. (C) Amplitudes of tail currents plotted as a function of the test potential and fitted to a Boltzmann function. (D) Steady-state inactivation of expressed currents in HEK293 cells showing normalized steady-state inactivation curves. The inset shows a portion of the voltage-clamp protocol and representative current traces from cells transfected with WT/Q738X-hERG. (n=6-10). *P<0.05, **P<0.01 vs. WT-hERG.

cells (Fig. 3Bi). In the cells expressing only WT channels, intense hERG-immunopositive labeling was observed at the plasma membrane (Fig. 3Bii, left column). Overlay of the 2 images demonstrated that there was partial co-localization of WT channels with calreticulin (Fig. 3Bii, middle and right columns). By contrast, the subcellular localization of the mutated Q738X channel was markedly perturbed (Fig. 3Biii, left column). No plasma membrane staining was visible; instead, a strong hERG-immunostaining was observed within the cytoplasm. Moreover, a clear co-localization of the mutant channel with calreticulin was observed (Fig. 3Biii, middle and right columns). When the WT and Q738X channels were co-expressed, the Q738X mutant was retained in the ER, while the WT protein was still transported to the membrane (Fig. 3Biv, left column). These channels displayed differential subcellular localization, as shown in the overlay image (Fig. 3Biv, middle and right columns).

Similar to other voltage-gated potassium channels, hERG subunits form functional channels as tetramers. To examine the possibility of heterotetrameric channel formation following co-expression, we examined the reciprocal co-immunoprecipitation of WT and Q738X. We co-transfected Flag-WT/Myc-Q738X, Flag-WT/WT or Myc-Q738X/Q738X into the HEK293 cells, and the co-assembly of the Flag-WT/Myc-Q738X channels was determined by immunoprecipitation using anti-Flag antibodies followed by western

blot analysis with anti-Myc antibodies or vice versa. As shown in Fig. 4A and B, Myc-tagged Q738X was not co-immunoprecipitated with Flag-tagged WT. Flag-tagged WT was co-immunoprecipitated with WT, but Myc-tagged Q738X was not co-immunoprecipitated with Q738X in the co-transfected cells (Fig. 4C and D). These results suggested that the Q738X mutant protein was synthesized as the 80-kDa immature form, but it was not converted to the mature form. Thus, the Q738X mutation appears to cause hERG channel dysfunction by disruption of the tetrameric assembly of the hERG channel.

Discussion

The hERG nonsense mutation described in the present study (Q738X) was previously identified in a Japanese LQTS family (7); the product of this mutation is the deletion of 86% of the C-terminal region of hERG channels. The Q738X mutation is positioned in the hERG C-terminus, with a deletion of 421 amino acids. The present study further investigated the biophysical properties and molecular characteristics of the Q738X mutation. Our results revealed that Q738X alone failed to form functional hERG channels, consistent with other reported C-terminus mutations [e.g., Q725X (5) and Y667X (11)]. These results are consistent with the finding that hERG proteins with a C-terminal truncation of 311 or more amino acid residues cannot form functional channels (12).

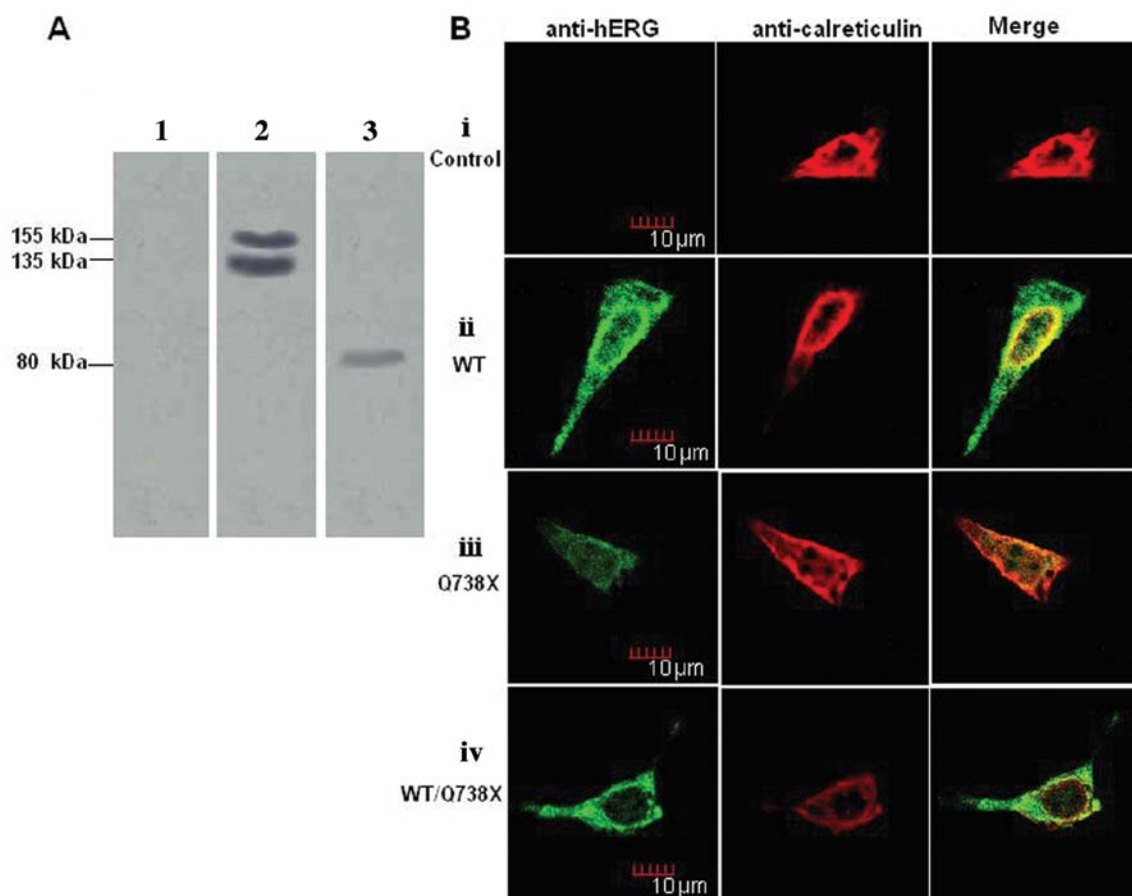


Figure 3. Expression of human *ether-a-go-go*-related gene (hERG) protein in HEK293 cells. (A) Expression of hERG protein as measured by western blot analysis. Lane 1, non-transfected cells; lane 2, wild-type (WT)-hERG-transfected cells; and lane 3, Q738X-hERG-transfected cells. (B) Expression of hERG protein in HEK293 cells. (i) No transfection, (ii) transfected with WT-hERG, (iii) transfected with Q738X-hERG, and (iv) transfected with WT/Q738X-hERG. Double immunofluorescence staining of hERG protein (left column, green); calreticulin, an endoplasmic reticulum (ER) marker protein (middle column, red); and overlay of the 2 images (right column).

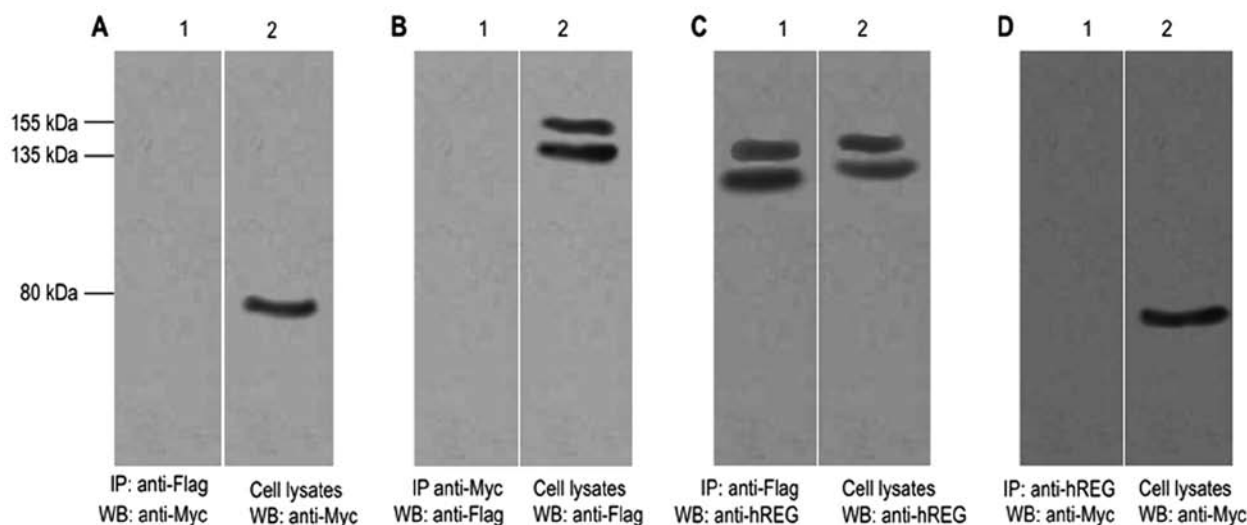


Figure 4. Co-assembly of the Q738X mutant with wild-type (WT)-human *ether-a-go-go*-related gene (hERG). (A and B) Flag-tagged WT-hERG was co-transfected with Myc-tagged Q738X-hERG into HEK293 cells. (C) Flag-tagged WT-hERG was co-transfected with WT-hERG into HEK293 cells. (D) Myc-tagged Q738X-hERG was co-transfected with Q738X-hERG into HEK293 cells. WB, western blot analysis.

Patients with LQT2, an inherited autosomal dominant disorder, can present with both normal and mutant alleles.

However, the severity of LQT may be associated with the nature of such mutations; for example, homozygous missense

mutations in hERG have been shown to be associated with a severe, early onset form of LQT (13). It is, therefore, believed that the interactions between mutant and normal hERG subunits may affect the pathogenesis of the LQT phenotype. In fact, studies have shown that the defective co-assembly of mutant and normal subunits into heterotetrameric channels allows wild-type subunits to establish homotetrameric channels, reducing the number of functional channels by 50% (14). However, even more importantly, the co-assembly of mutant subunits with wild-type subunits, forming heterotetrameric channels, may produce dysfunctional channels that reduce hERG channel function by more than 50%, thereby exhibiting a dominant-negative effect (5). Our patch clamp experiments revealed that the co-expression of WT/Q738X hERG (at a 1:1 ratio) reduced hERG current densities by approximately 50%, which decreased gradually with increasing amounts of Q738X cDNA. In addition, we showed that Q738X mutant subunits did not co-assemble with wild-type subunits to form heterotetrameric channels using co-immunoprecipitation techniques. These results strongly indicated that the disruption of the tetrameric assembly of mutant channels may play an important role in the failure of Q738X to reach the plasma membrane.

The biological properties of hERG channels may be differentially altered by mutations in different regions of the protein (15). The intracellular C terminal region of the channel, for example, is critical to maintaining the biophysical properties of hERG (16). Additionally, certain truncations of hERG protein may result in trafficking problems and dysfunction of the hERG channel, blocking the generation of hERG currents (17), and other mutations may still permit the formation of functional channels (18). Certain studies have identified specific regions and mutations that affect hERG function. For example, Akhavan *et al* (19) found that the region within residues 860–899 is essential for the proper trafficking of hERG protein. Additionally, Lees-Miller *et al* (20) demonstrated that a mutation in R863 (R863X) resulted in the failure of the protein to undergo proper trafficking to the plasma membrane, thereby preventing the formation of functional channels. Finally, Gong *et al* (5) investigated the Q725X mutation and found that this mutation interfered with the proper tetrameric assembly of hERG channels, leading to dysfunction of the channel. The R1014X mutation, however, did allow the formation of a tetrameric structure, but still resulted in hERG channel dysfunction due to problems with trafficking of mutant subunits. Thus, these previous studies effectively demonstrated that the trafficking and maturation of the hERG channel is mediated by the C-terminal region of the hERG protein.

In conclusion, the findings of the present study demonstrate that the functional loss caused by Q738X mutation in hERG K⁺ channel may be attributed to the disruption of the tetrameric assembly.

Acknowledgements

The present study was supported by grants from the National Natural Science Foundation of China (no. 81200138) and the Key Technologies R&D Program of Henan Province (no. 92102310225).

References

- Priori SG, Barhanin J, Hauer RN, Haverkamp W, Jongasma HJ, Kleber AG, McKenna WJ, Roden DM, Rudy Y, Schwartz K, Schwartz PJ, Towbin JA and Wilde AM: Genetic and molecular basis of cardiac arrhythmias: impact on clinical management parts I and II. *Circulation* 99: 518–528, 1999.
- Craft TM: Torsade de pointes after astemizole overdose. *Br Med J (Clin Res Ed)* 292: 660, 1986.
- Mathews DR, McNutt B, Okerholm R, Flicker M and McBride G: Torsades de pointes occurring in association with terfenadine use. *JAMA* 266: 2375–2376, 1991.
- Anderson CL, Delisle BP, Anson BD, Kilby JA, Will ML, Tester DJ, Gong Q, Zhou Z, Ackerman MJ and January CT: Most LQT2 mutations reduce Kv11.1 (hERG) current by a class 2 (trafficking-deficient) mechanism. *Circulation* 113: 365–373, 2006.
- Gong Q, Keeney DR, Robinson JC and Zhou Z: Defective assembly and trafficking of mutant HERG channels with C-terminal truncations in long QT syndrome. *J Mol Cell Cardiol* 37: 1225–1233, 2004.
- Perrin MJ, Subbiah RN, Vandenberg JI and Hill AP: Human *ether-a-go-go* related gene (hERG) K⁺ channels: function and dysfunction. *Prog Biophys Mol Biol* 98: 137–148, 2008.
- Yasuda S, Hiramatsu S, Odashiro K, Maruyama T, Tsuji K and Horie M: A family of hereditary long QT syndrome caused by Q738X HERG mutation. *Int J Cardiol* 144: 69–72, 2010.
- Guo J, Han SN, Liu JX, Zhang XM, Hu ZS, Shi J, Zhang LR, Zhao ZZ and Zhang Z: The action of a novel fluoroquinolone antibiotic agent ofloxacin hydrochloride on human-*ether-a-go-go*-related gene potassium channel. *Basic Clin Pharmacol Toxicol* 107: 643–649, 2010.
- Han S, Zhang Y, Chen Q, Duan Y, Zheng T, Hu X, Zhang Z and Zhang L: Fluconazole inhibits hERG K⁺ channel by direct block and disruption of protein trafficking. *Eur J Pharmacol* 650: 138–144, 2011.
- Takemasa H, Nagatomo T, Abe H, Kawakami K, Igarashi T, Tsurugi T, Kabashima N, Tamura M, Okazaki M, Delisle BP, January CT and Otsuji Y: Coexistence of hERG current block and disruption of protein trafficking in ketoconazole-induced long QT syndrome. *Br J Pharmacol* 153: 439–447, 2008.
- Paulussen A, Yang P, Pangalos M, Verhasselt P, Marrannes R, Verfaillie C, Vandenberg I, Crabbe R, Konings F, Luyten W and Armstrong M: Analysis of the human KCNH2(hERG) gene: identification and characterization of a novel mutation Y667X associated with long QT syndrome and a non-pathological 9 bp insertion. *Hum Mutat* 15: 483–487, 2000.
- Aydar E and Palmer C: Functional characterization of the C-terminus of the human *ether-a-go-go*-related gene K⁺ channel (HERG). *J Physiol* 534: 1–14, 2001.
- Johnson WH Jr, Yang P, Yang T, Lau YR, Mostella BA, Wolff DJ, Roden DM and Benson DW: Clinical, genetic, and biophysical characterization of a homozygous HERG mutation causing severe neonatal long QT syndrome. *Pediatr Res* 53: 744–748, 2003.
- Keating MT and Sanguinetti MC: Molecular genetic insights into cardiovascular disease. *Science* 272: 681–685, 1996.
- Tseng GN: I_{Kr}: the hERG channel. *J Mol Cell Cardiol* 33: 835–849, 2001.
- Jenke M, Sanchez A, Monje F, Stuhmer W, Weseloh RM and Pardo LA: C-terminal domains implicated in the functional surface expression of potassium channels. *EMBO J* 22: 395–403, 2003.
- Ficker E, Thomas D, Viswanathan PC, Dennis AT, Priori SG, Napolitano C, Memmi M, Wible BA, Kaufman ES, Iyengar S, Schwartz PJ, Rudy Y and Brown AM: Novel characteristics of a misprocessed mutant HERG channel linked to hereditary long QT syndrome. *Am J Physiol Heart Circ Physiol* 279: H1748–H1756, 2000.
- Yao Y, Teng S, Li N, Zhang Y, Boyden PA and Pu J: Aminoglycoside antibiotics restore functional expression of truncated HERG channels produced by nonsense mutations. *Heart Rhythm* 6: 553–560, 2009.
- Akhavan A, Atanasiu R, Noguchi T, Han W, Holder N and Shrier A: Identification of the cyclic-nucleotide-binding domain as a conserved determinant of ion-channel cell-surface localization. *J Cell Sci* 118: 2803–2812, 2005.
- Lees-Miller JP, Duan Y, Teng GQ, Thorstad K and Duff HJ: Novel gain-of-function mechanism in K⁺ channel-related long-QT syndrome: altered gating and selectivity in the HERG1 N629D mutant. *Circ Res* 86: 507–513, 2000.